Proceedings of the Fourth Lunar Science Conference
(Supplement 4, *Geochimica et Cosmochimica Acta*)
Vol. 3, pp. 2793–2802

Distribution of ^{222}Rn and ^{210}Po on the lunar surface as observed by the alpha particle spectrometer

PAUL J. BJORKHOLM, LEON GOLUB, and PAUL GORENSTEIN

American Science and Engineering, 955 Massachusetts Avenue, Cambridge, Mass. 02139

Abstract—The distribution of ^{222}Rn and her daughter products has been observed from orbit during the Apollo 15 and Apollo 16 missions. Decays of ^{222}Rn were observed locally over the crater Aristarchus and more generally over Oceanus Procellarum and Mare Imbrium. Decays of ^{210}Po (a delayed daughter of ^{222}Rn) were observed over most of the eastern hemisphere on both missions. All observations indicate a lack of radioactive equilibrium between ^{222}Rn and ^{210}Po implying a time dependent process for the production of radon at the lunar surface. In addition, the ^{210}Po shows a remarkable correlation with the Mare edges.

INTRODUCTION

RADON-222 is a radioactive noble gas which is produced during the decay of uranium. Because it is a noble gas, under certain conditions it may diffuse through the lunar regolith and reach the surface before decaying by alpha particle emission. The alpha particle spectrometers aboard the Apollo 15 and 16 spacecrafts were designed to detect and identify the alpha particles emitted by ^{222}Rn and her daughter products during decay. The theory and experimental techniques have been described previously by Gorenstein and Bjorkholm (1972). The observed signal strengths relate to the concentration of the parent uranium and the depth from which radon may reach the surface prior to decay.

In order to fully appreciate the observations one must have at least some understanding of the processes involved in transporting radon to the lunar surface. Therefore included below is a brief summary of these possible processes. The ultimate source of the observed radon is the natural radioactive decay chain of uranium. The radon is produced at the site of its parents, i.e., within mineral grains. In order for the radon to reach the surface two distinct processes must occur. First the radon must be released to the voids between the mineral grains. This process is commonly referred to as emanation. Emanation can occur by diffusion within the solid grains or by recoil out of the grain from the alpha decay of its parent. Neither process is expected to be efficient on the lunar surface. In particular, to have the recoil process be efficient one requires a stopping medium between the mineral grains. On earth the atmosphere provides some stopping power. The lack of a lunar atmosphere must significantly reduce the efficiency of this process. One can postulate other mechanisms to allow some residual emanation even without any intergrain stopping power available but these effects will be very weak. Once a neutral radon atom is in the lunar regolith it must migrate to the surface to be observable by the spectrometer. This can occur by a random walk

through the regolith or by transport within some other medium passing through the regolith.

Any spatial and/or temporal variation in the observed signal at the lunar surface is a reflection of the variations in these processes of emanation and migration. Therefore any mechanisms postulated to describe these processes must fit the observed boundary conditions, i.e., the data to be presented below.

OBSERVATIONS

The observed data can be grouped in several different ways. They will be discussed here by considering first the general trends and then the specific correlation with lunar features. Observations of ^{210}Po and ^{222}Rn will be discussed simultaneously. The important point to bear in mind is that the decay of ^{222}Rn represents activity that was occurring at the time of observation. Decay of ^{210}Po represents activity that is caused by ^{222}Rn reaching the lunar surface prior to the observation (from about 10 days to 60 years). Therefore the observed ^{222}Rn to ^{210}Po ratio is an indication of the secular history of the radon emanation.

GLOBAL TRENDS

Figure 1 shows the observed count rate for ^{222}Rn (plus her two prompt daughters) as a function of longitude for the Apollo 15 ground track. The data are displayed in four panels, each containing 90° of lunar longitude, the top panel starting at 0° and proceeding to the East (towards Mare Crisium). There is a background level, and the middle two panels (the lunar farside) are consistent with this background level (the dashed line represents the whole moon average). The average count rate in each quadrant is indicated on the figure. While the ability to observe detailed structure in these data is limited by the counting statistics, there is an increase in the amount of ^{222}Rn observed over the western quadrant (Oceanus Procellarum and Mare Imbium) and to a lesser extent over the eastern quadrant (Maria Serenitatis, Tranquillitatis, Fecunditatis, and Crisium). The signal bin labeled "Arist." (for Aristarchus) in Fig. 1 has been excluded from the average and will be discussed below. The general trend of the count rate is in agreement with the observed uranium and thorium concentrations over the same region (Metzger *et al.*, 1972).

The ^{210}Po distributions show a considerably larger spatial variation and are shown in Figs. 2 (Apollo 15) and 3 (Apollo 16). The Apollo 15 ^{210}Po distribution (including a cosmic ray background) shows an increase in signal between 40°E and 180°E. The average count rate between 40°E and 180°E is 0.072 ± 0.002 counts/sec and 0.062 ± 0.001 counts/sec elsewhere. The excess count rate between 40°E and 180°E corresponds to a ^{210}Po decay rate of $(4.6 \pm 1.4) \times 10^{-3}$ disintegration/cm^2-sec (dis/cm^2-sec).

The Apollo 16 ^{210}Po distribution (Fig. 3) shows an even more striking spatial variation. In general there is an increase starting at 90°W (Oceanus Procellarum) continuing across the front side of the moon and reaching a maximum over Mare

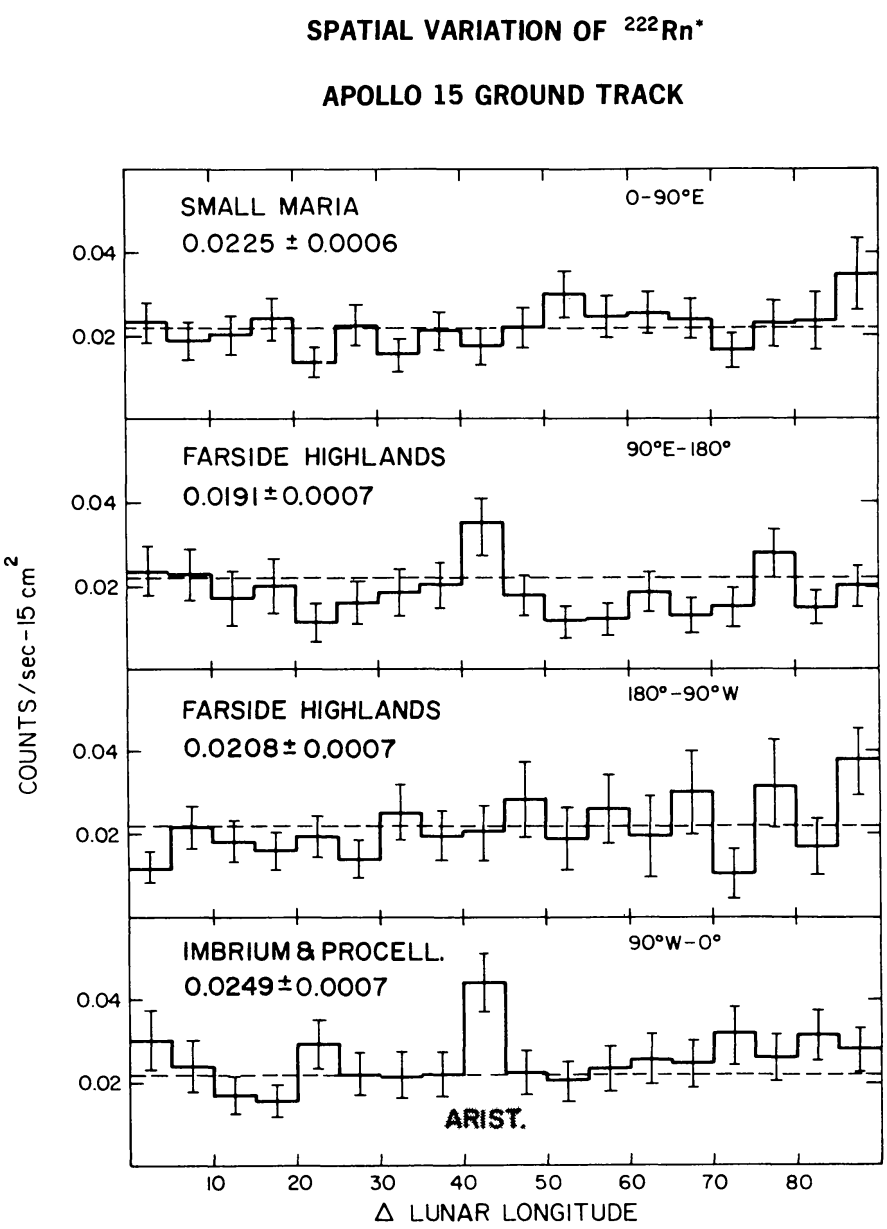

Fig. 1. Distribution of the observed ^{222}Rn (plus two prompt daughters) count rate as a function of longitude for the Apollo 15 ground track. The dashed line represents the average decay rate for the total observed data (including background). The average count rate for each quadrant is indicated in each panel. The error bars are counting statistics only.

Fecunditatis and Mare Smythii. Beyond this point the rate drops dramatically and remains low over the lunar farside. Because the Apollo 16 mission had a fairly low inclination orbit, the statistics are sufficient to generate a two-dimensional display. This is shown in Fig. 4. Here the data are grouped into $10° \times 10°$ bins and displayed relative to the background counting rate obtained from data taken with the

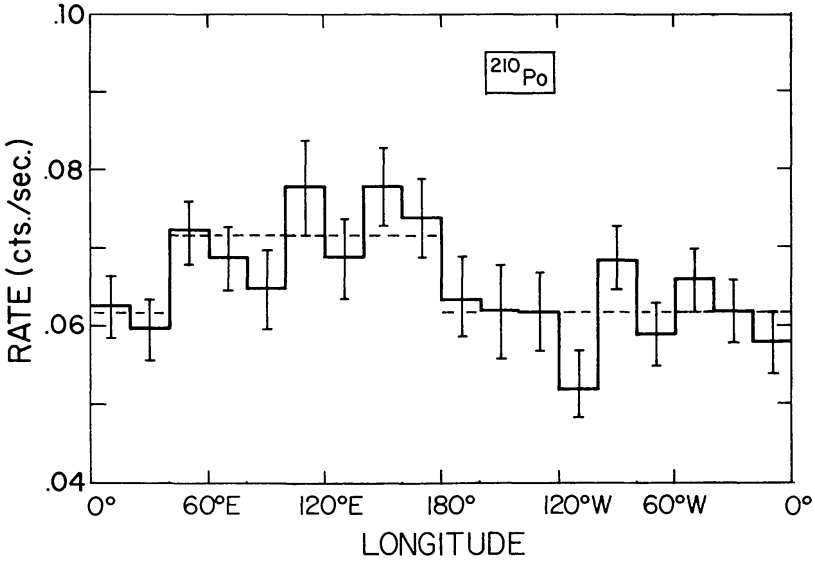

Fig. 2. Observed count rate at the energy of lunar ^{210}Po as a function of longitude for the Apollo 15 ground track. The dashed lines represent the average count rate in two regions (40–180°E, and 0–40°E plus 180°W–0°). The error bars are counting statistics only. The decay rate at the lunar surface in dis/cm^2-sec is 0.43 times the experiment count rate.

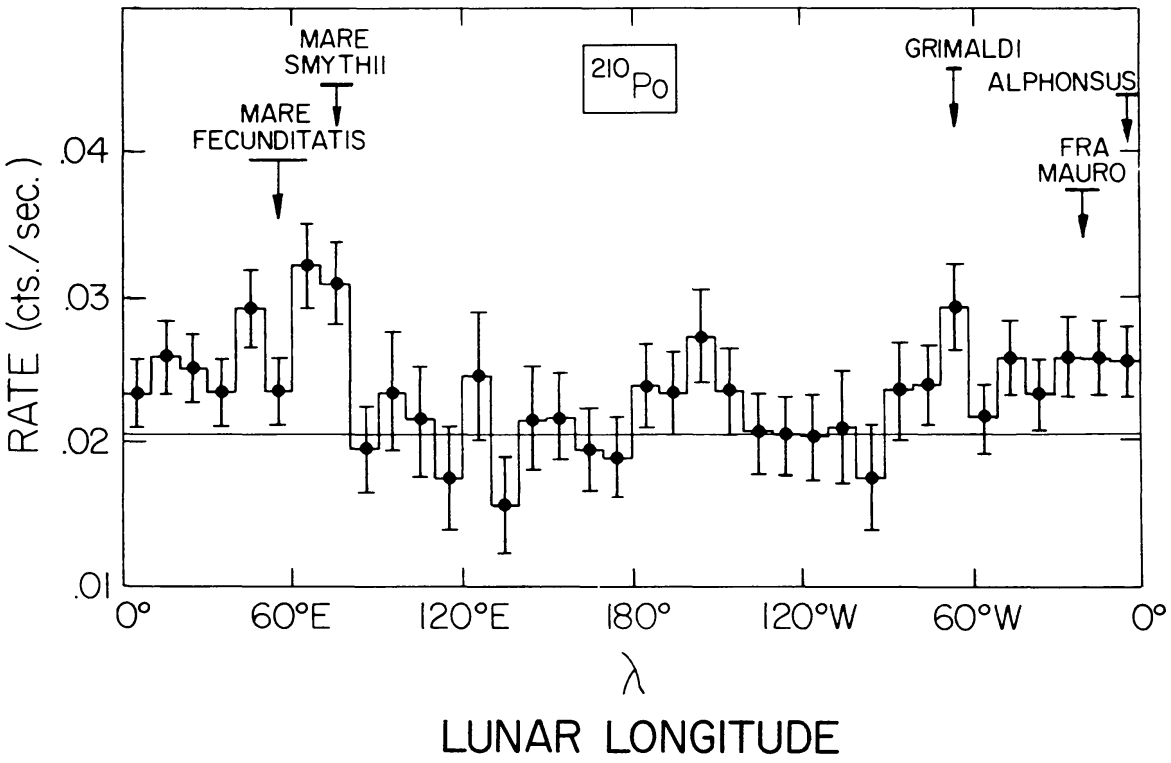

Fig. 3. Observed count rate at the energy of lunar ^{210}Po as a function of lunar longitude for the Apollo 16 ground track. The solid line is the observed background level in the detectors. Location information is included for reference only. The error bars are counting statistics only. The decay rate at the lunar surface in dis/cm^2-sec is 0.36 times the experiment count rate.

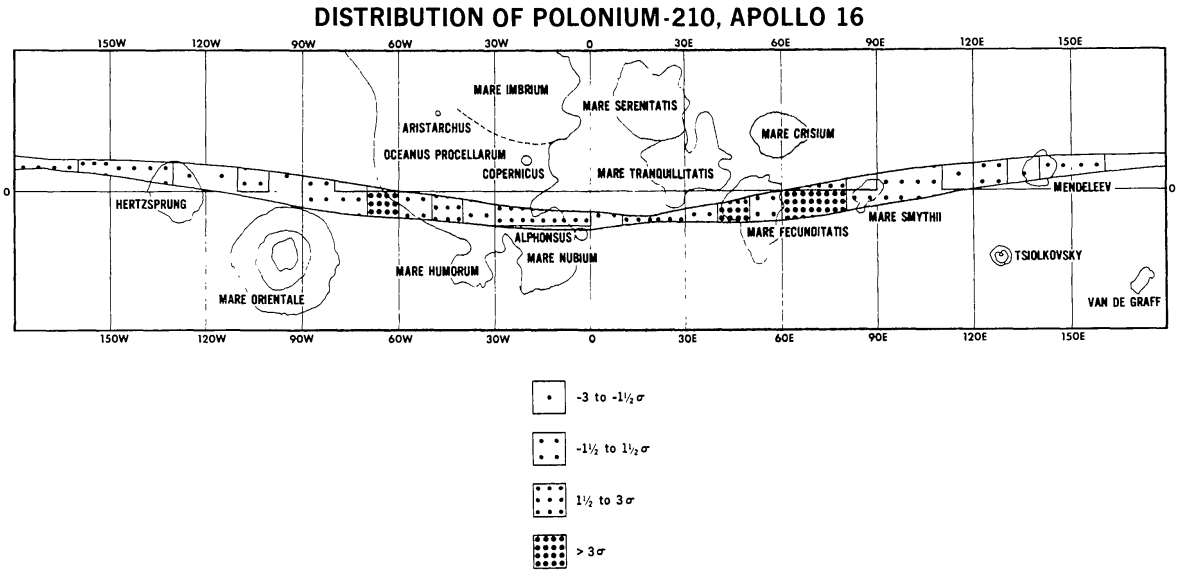

Fig. 4. Observed count rate of lunar ^{210}Po displayed on a schematic lunar map. The data are grouped in $10° \times 10°$ bins. The symbols are given on the figure and refer to standard deviations (counting statistics only) above (or below) the measured background level.

instrument in a non-lunar orientation. These data are discussed in more detail in Bjorkholm *et al.* (1973).

The observed ^{210}Po count rates, relative to background, from both missions are shown overlayed on a lunar map in the frontispiece. Because the amount of data gathering time (and therefore statistical accuracy) varies from region to region, the data are displayed in terms of the number of standard deviations (counting statistics only) above or below background. In the region of ground track overlap between the two missions, the data are combined. Within these regions the observed count rates above background from the two missions were in statistical agreement.

The observed ^{222}Rn and ^{210}Po decay rates are not in radioactive equilibrium. This implies that the processes causing the variation are time varying.

Correlations with Topographical Features

The ^{222}Rn distribution as a function of longitude (Fig. 1) showed one 5° bin which was significantly in excess of the surrounding region. This corresponded to the region including the crater Aristarchus. Figure 5 shows a subset of these data, including only those times when Aristarchus was within the instrument's field of view, overlayed on a photograph of the moon. The dashed line represents the average ground track during this time interval and the solid line is the ^{222}Rn count rate referenced to the dashed line. There is an increase in count rate over the crater Aristarchus which is 4.3 standard deviations (σ) with respect to the mean counting rate for the moon. Based on Poisson counting statistics the probability that this increase is due to a statistical fluctuation coincident with Aristarchus is 10^{-4}. The excess over background is $(10.1 \pm 3.3) \times 10^{-3}$ dis/cm^2-sec. The increase is

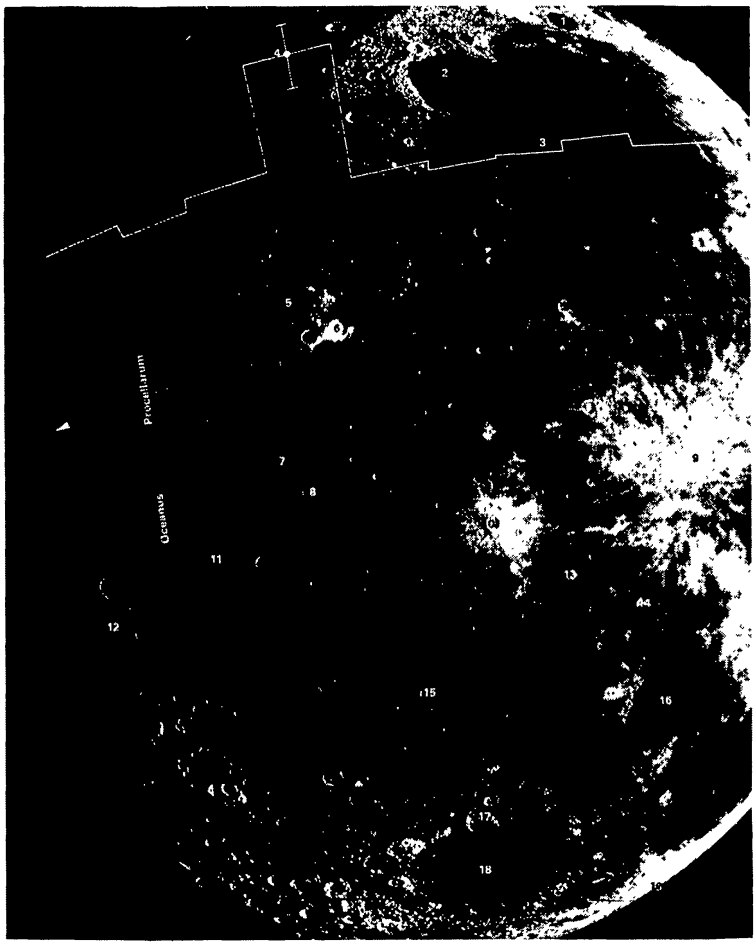

Fig. 5. The observed count rate of ^{222}Rn (plus two prompt daughters) superimposed on a photograph of the moon. The dashed line represents the average ground track for that portion of the Apollo 15 mission when the crater Aristarchus was within the alpha particle spectrometer's field of view. The data are referenced to this line.

centered over the crater Aristarchus, but the statistics are insufficient to distinguish among Aristarchus, Schröter's Valley, and Cobrahead as the center of the effect. These data are discussed in more detail in Gorenstein and Bjorkholm (1973).

A similar feature was seen in the Apollo 16 ^{210}Po data. Here we see a very strong increase over the crater Grimaldi. This is shown in Fig. 6. The dashed line represents the average ground track and the data are plotted with respect to this line assuming it to be the background level. The ^{210}Po decay rate directly over the crater Grimaldi exceeds the background rate by $(3.3 \pm 1.1) \times 10^{-3}$ dis/cm^2-sec.

Another example of this type of spatially localized concentration of ^{210}Po is shown in Fig. 7. The count rate for ^{210}Po decays is shown as the ground track crosses Mare Fecunditatis. The highlands to either side of the Mare, the edges of the Mare, and the central region are indicated on the figure. The solid line is the background level. The observed rate falls to background levels on either side of

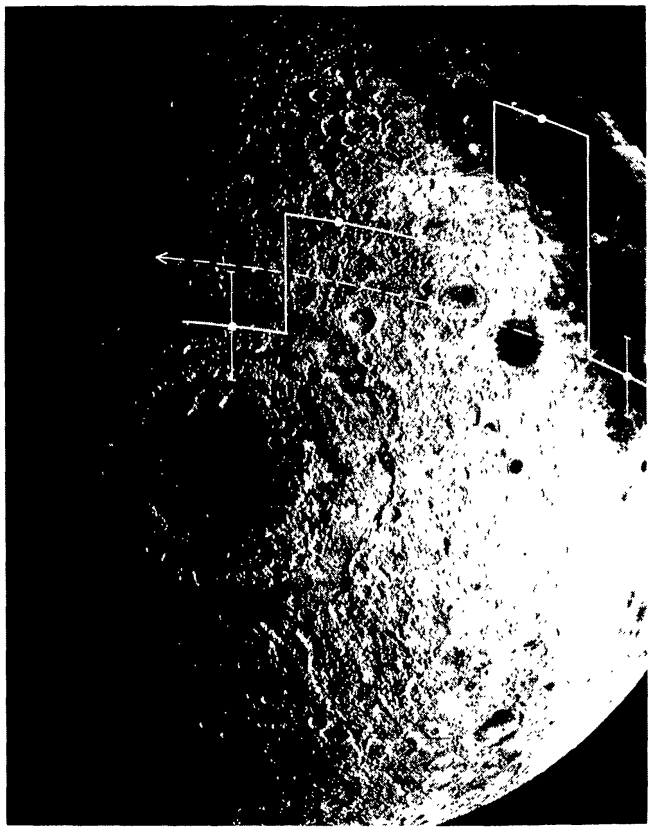

Fig. 6. The observed ^{210}Po count rate superimposed on a photograph of the moon. The dashed line represents the average ground track and is used to represent the background counting level. The crater directly beneath the local increase in count rate is the crater Grimaldi.

the Mare and in the center. The increase is associated strictly with the edges.

Figure 8 shows the energy spectrum observed over the edges (solid line) and over the center (dashed line) of the Mare. The lower panel shows the differential spectrum (edge—center). This clearly shows that the excess is due to ^{210}Po and shows that radioactive equilibrium does not exist between ^{222}Rn and ^{210}Po at the time of observation.

While Mare Fecunditatis shows this effect most dramatically, it is not unique. Table 1 gives the count rate at all observed Mare edges relative to background. The data are divided into five categories based on the distance from the Mare edge. The terms "In" and "Out" are used to refer to data taken over the Mare surface and over the surrounding highlands respectively. Certain entries are indicated as "no data" either because the ground track did not cover that region or because the Mare itself is less than 500 kilometers in diameter. The data from the two missions for the same Mare need not agree since different portions of the Mare were observed. All of the observed Maria, with the exception of Serenitatis, show an enhanced decay rate for ^{210}Po at their edges. In particular, Maria Fecunditatis and Crisium show this effect most dramatically.

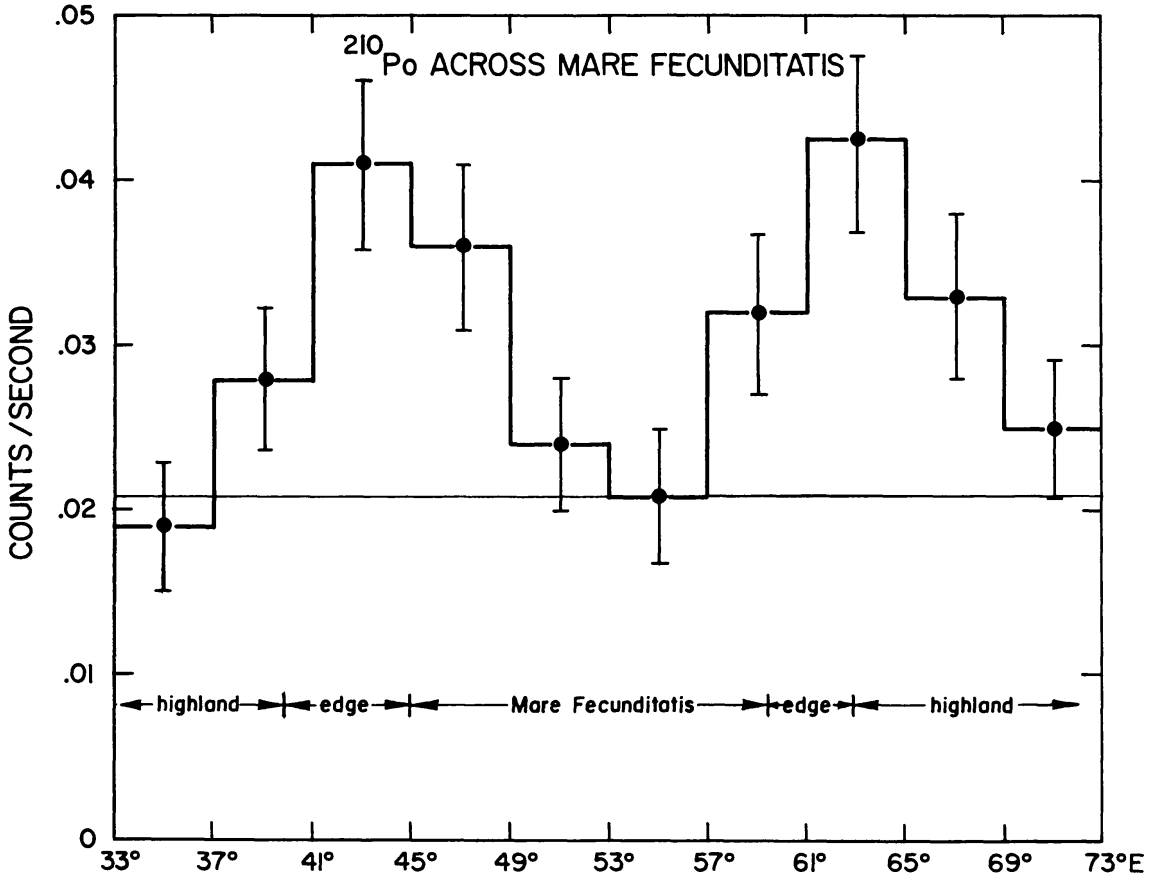

Fig. 7. The observed ^{210}Po count rate as a function of longitude as the ground track crossed Mare Fecunditatis (Apollo 16). The solid line is the observed background level. The highland, mare, and edge regions are indicated. The finite width to the "edge" is caused by the oblique crossing of the Mare-highland interface by the ground track.

DISCUSSION

The observed ^{222}Rn and ^{210}Po distributions over the lunar surface are remarkably inhomogeneous. Variations in decay rate occur over distances of five degrees or less and most of the variations can be directly correlated with lunar surface features. Further, even though the data obtained over Aristarchus indicated that ^{222}Rn was in radioactive equilibrium with her prompt daughters, none of the observed data indicated radioactive equilibrium between ^{222}Rn and ^{210}Po, her delayed daughter. This implies that the processes responsible for radon transportation to the lunar surface are also time varying.

The spatial and implied temporal variations of the observed signals require a similar type of variation for the radon transport mechanisms in the lunar regolith. Any proposed mechanisms for radon transport must then be capable of producing these types of observations. On the other hand, the spatial correlations are so specific that a study of other lunar surface phenomena might yield some insight into possible radon transport mechanisms. This will be considered further in the following paper.

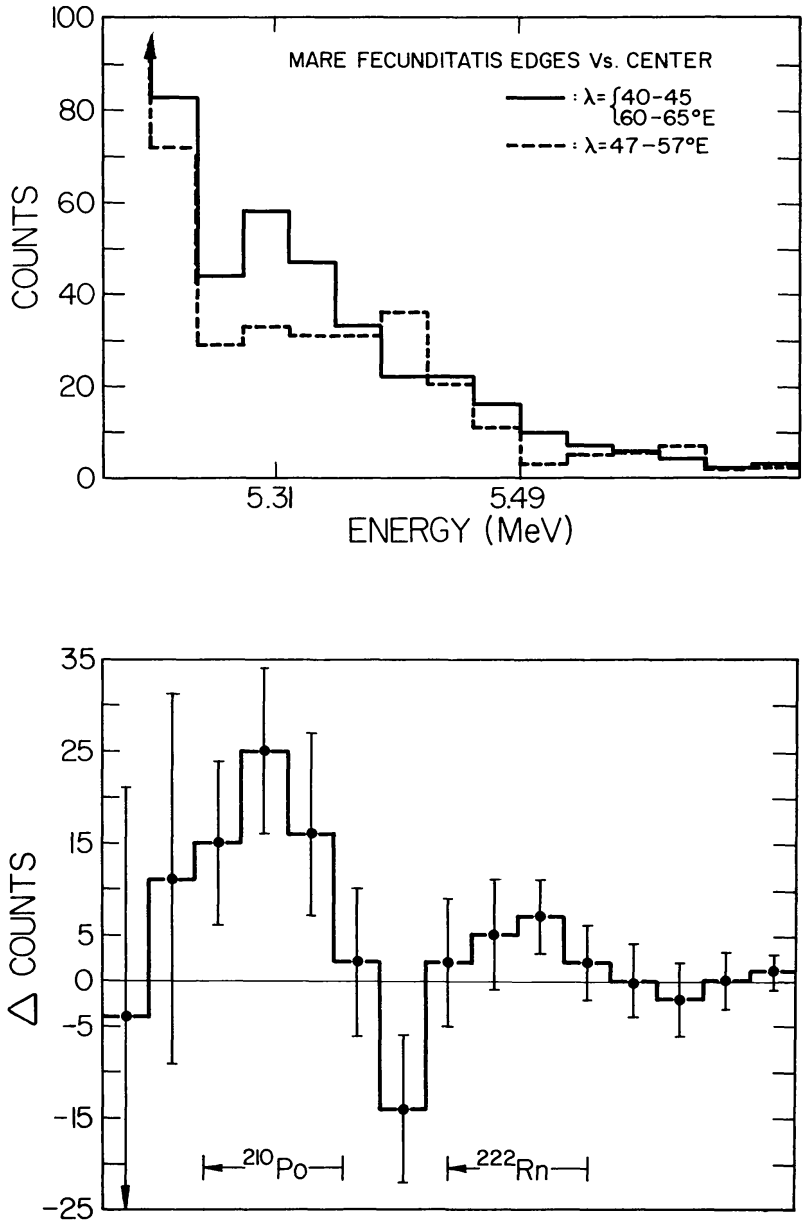

Fig. 8. Top panel: Energy spectra observed at Mare Fecunditatis. The solid line is data obtained over the edges and the dashed line is data obtained over the center of the Mare. Bottom panel: The (time normalized) differential energy spectrum (edge—center). Any energy region having a higher count rate over the edge region will appear as a positive excess in this spectrum. The excess due to ^{210}Po decays is clearly visible. The ^{222}Rn excess is of marginal statistical significance but the ratio between the ^{210}Po and ^{222}Rn excesses establishes secular variability.

Table 1. ^{210}Po decay rate at Maria edges[a].

Mare	In: 200–350 km	In: 75–200 km	Edge ±75 km	Out: 75–200	Out: 200–350 km
A. Apollo 15					
Fecunditatis	−0.1±4.3	11.1±4.4	12.5±3.5	8.1±5.8	no data
Crisium	no data	no data	20.1±5.2	4.1±5.6	−5.6±8.0
Smythii	no data	−5.6±10.1	14.1±4.2	9.0±6.3	6.2±7.5
Procellarum	−7.7±5.3	1.5±3.8	5.4±4.1	4.0±4.2	−6.7±6.2
Imbrium	3.4±4.5	2.3±4.2	4.6±3.1	no data	no data
Tranquillitatis	2.1±6.3	−7.7±2.8	8.0±2.6	no data	no data
Serenitatis	no data	5.1±4.4	4.0±2.9	4.5±3.4	no data
Total—Apollo 15	−0.1±2.5	1.0±1.6	8.4±1.3	5.3±2.1	−1.9±4.1
B. Apollo 16					
Fecunditatis	no data	6.8±2.1	19.5±3.1	7.1±2.8	8.3±7.1
Smythii	no data	3.4±4.7	9.5±3.1	10.9±3.0	7.5±5.3
Tranquillitatis	no data	no data	11.6±3.8	4.7±2.4	9.3±2.7
Nubium	no data	no data	11.5±3.6	8.1±2.8	3.9±3.4
Cognitum	no data	6.6±2.8	11.2±2.7	7.3±3.7	no data
Total—Apollo 16	no data	6.5±1.7	13.3±1.5	7.7±1.3	7.6±1.9
Total A15 & A16	−0.1±2.5	2.9±1.3	9.8±1.0	6.7±1.2	4.9±1.8

[a]Rates are $\times 10^{-3}$ cts/sec = 0.36×10^{-3} dis/cm^2-sec at the lunar surface.

REFERENCES

Bjorkholm P., Golub L., and Gorenstein P. (1973) Detection of a non-uniform distribution of ^{210}Po on the Moon with the Apollo 16 alpha particle spectrometer. *Science* **180**, 957–959.

Gorenstein P. and Bjorkholm P. (1972) Observation of lunar radon emanation with the Apollo 15 alpha particle spectrometer. *Proc. Third Lunar Sci. Conf., Geochim. Cosmochim. Acta,* Suppl. 3, Vol. 3, pp. 2179–2187. MIT Press.

Gorenstein P. and Bjorkholm P. (1973) Detection of radon emanation from the crater Aristarchus by the Apollo 15 alpha particle spectrometer. *Science* **179**, 792–794.

Metzger A. E., Trombka J. I., Peterson L. E., Reedy R. C., and Arnold J. R. (1972) A first look at the lunar orbital gamma-ray data. *Proc. Third Lunar Sci. Conf., Geochim. Cosmochim. Acta,* Suppl. 3, Vol. 3, frontispiece. MIT Press.